

Diagrammatic Design of Ansätze for Quantum Chemistry



Ayman El Amrani

St. John's College

A thesis submitted for the Honour School of Chemistry

Part II 2024

Pour ma mère et mon père.
Merci de m'avoir amené jusqu'ici.

Acknowledgements

Thank you Thomas Cervoni for your constant motivation and support.

Thank you David Tew and Stefano Gogioso for your patient supervision.

Thank you Razin Shaikh, Boldizsár Poór, Richie Yeung and Harny Wang for always finding the time to answer my questions.

Thank you to my friends and family for supporting me during this unconventional Master's.

Summary

A central challenge in computational quantum chemistry is the accurate simulation of fermionic systems. At the heart of these calculations lies the need to solve the Schrödinger equation to determine the many-electron wavefunction. An exact solution to this problem scales exponentially with the number of electrons. Classical computers struggle to store the increasingly large wavefunctions making this problem computationally intractable in many cases. In contrast, gate-based quantum computing presents a promising solution, offering the potential to represent electronic wavefunctions with polynomially scaling resources [1]. In other words, quantum computers are a natural tool of choice for simulating processes that are inherently quantum [2].

In the last two decades many advancements in quantum computing have been made in both hardware and software bringing us closer to being able to simulate molecular systems. Despite these advancements, we remain in the so-called Noisy Intermediate Scale Quantum (NISQ) era, characterised by challenges such as poor qubit fidelity, low qubit connectivity and limited coherence times. The NISQ era represents a transitional phase in quantum computing, where quantum devices are not yet error-corrected but are still capable of performing computations beyond the reach of classical computers. Overcoming the limitations of the NISQ era is crucial for realising the full potential of quantum computing in various fields, including quantum chemistry and materials science.

The Variational Quantum Eigensolver (VQE) algorithm is a method used to estimate the ground state energy of a molecular Hamiltonian by preparing a trial wavefunction,

calculating its energy, and optimising the wavefunction parameters classically until the energy converges to the optimal approximation for the ground state energy [3]. It is recognised as a leading algorithm for quantum simulation on NISQ devices due to its reduced resource requirements in terms of qubit count and coherence time [4].

This thesis extends methods developed by Richie Yeung [2] for the preparation and analysis of parametrised quantum circuits, and applies them to ansätze representing fermionic wavefunctions. We are concerned with two main questions along this theme. Firstly, can we use the ZX calculus [cite] to gain insights about the structure of the unitary product ansatz in the context of variational algorithms for quantum chemistry? Secondly, in the context of NISQ devices, can we use these insights to build better ansätze, with reduced circuit depth and more efficient resources?

Contents

1	Background	1
1.1	Fermionic Simulation Scheme	2
1.2	Unitary Coupled Cluster	3
1.3	Fermion-Qubit Encodings	7
1.4	DISCO-VQE	10
2	Phase Gadgets	12
2.1	Phase Gadgets	12
2.2	Pauli Gadgets	12
2.3	Commutation Relations	12
3	Pauli Gadgets	13
4	Controlled Rotations	14
4.1	Singly-Controlled Rotations	14
4.2	Doubly-Controlled Rotations	14
4.3	Triply-Controlled Rotations	14
5	ZxFermion Package	15
5.1	Creating Gadgets	15
5.2	Creating Circuits of Gadgets	15
5.3	Pauli & Clifford Algebra	15
5.4	Architecture-Aware Circuit Extraction	15

Contents

Appendices

Bibliography

17

Chapter 1

Background

1. Background

1.1 Fermionic Simulation Scheme

1. Map some fermionic state, usually in the occupation number representation to a qubit state.
2. This mapping must be done in such a way as to preserve the fermionic anti-commutation relations, and hence preserve Pauli antisymmetry.
3. Common fermionic-qubit mappings include Jordan-Wigner and Bravyi-Kitaev.
4. We then act on the qubit state with a unitary operator that represents a fermionic operator.
5. The resulting qubit state is then decoded to yield the resultant fermionic state.
6. A successful simulation scheme is one that reproduces the action of the fermionic operator

1. Background

1.2 Unitary Coupled Cluster

Second Quantisation

In second quantisation, wavefunctions are represented in the occupation number representation.

$$|\psi\rangle = |f_{n-1} \dots f_0\rangle \quad \text{where } f_j \in 0, 1$$

Where $|\psi\rangle$ represents a Slater determinant usually constructed from Hartree-Fock spin orbitals.

This means that given n spin-orbitals, there exist 2^n electronic basis states.

$$|\psi\rangle = |0 \dots 10\rangle = \begin{pmatrix} 0 \\ 1 \\ \vdots \\ \vdots \\ \vdots \\ 0 \end{pmatrix}$$

Fermionic interactions can be represented in terms of the creation and annihilation operators a_j^\dagger and a_j .

Consider the excitation of an electron in the lowest spin-orbital to the second spin-orbital.

$$|\psi_1\rangle \rightarrow |\psi_2\rangle \\ a_2^\dagger a_1 |001\rangle = |010\rangle$$

Importantly, due to the exchange anti-symmetry of fermions, the action of the creation/annihilation operators introduces a phase to the electronic wavefunction.

$$\begin{aligned} a_j^\dagger |f_{n-1} \dots f_{j+1}, 0, f_{j-1} \dots f_0\rangle &= (-1)^{\sum_{s=0}^{j-1} f_s} |f_{n-1} \dots f_{j+1}, 1, f_{j-1} \dots f_0\rangle \\ a_j^\dagger |f_{n-1} \dots f_{j+1}, 1, f_{j-1} \dots f_0\rangle &= \vec{0} \\ a_j |f_{n-1} \dots f_{j+1}, 1, f_{j-1} \dots f_0\rangle &= (-1)^{\sum_{s=0}^{j-1} f_s} |f_{n-1} \dots f_{j+1}, 0, f_{j-1} \dots f_0\rangle \\ a_j |f_{n-1} \dots f_{j+1}, 0, f_{j-1} \dots f_0\rangle &= \vec{0} \end{aligned}$$

1. Background

The phase introduced depends on the **parity** of the spin-orbitals preceding spin-orbital j .

In the second-quantisation, this anti-symmetry is expressed in terms of the anti-commutation of creation and annihilation operators.

$$\begin{aligned}\{\hat{a}_j, \hat{a}_k\} &= \hat{a}_j \hat{a}_k + \hat{a}_k \hat{a}_j = 0 \\ \{\hat{a}_j^\dagger, \hat{a}_k^\dagger\} &= \hat{a}_j^\dagger \hat{a}_k^\dagger + \hat{a}_k^\dagger \hat{a}_j^\dagger = 0 \\ \{\hat{a}_j, \hat{a}_k^\dagger\} &= \hat{a}_j \hat{a}_k^\dagger + \hat{a}_k^\dagger \hat{a}_j = \delta_{jk} \hat{1}\end{aligned}$$

In fact, we find that the phase factor discussed in the previous section is automatically kept track of by these relations.

The Hamiltonian in second quantisation can also be expressed in terms of the creation and annihilation operators.

$$\hat{H} = \sum_{ij} h_{ij} \hat{a}_i^\dagger \hat{a}_j + \frac{1}{2} \sum_{ijkl} h_{ijkl} \hat{a}_i^\dagger \hat{a}_j^\dagger \hat{a}_k \hat{a}_l + h_{\text{Nu}}$$

Where h_{ij} (one-electron overlap integral) and h_{ijkl} (two-electron overlap integral) are computed classically.

Coupled Cluster & Unitary Coupled Cluster

Within the traditional coupled-cluster framework, the ground electronic state is prepared by applying the CC operator to a reference state (usually Hartree-Fock).

$$|\psi\rangle = e^{\hat{T}} |\phi_0\rangle$$

Where \hat{T} is the cluster excitation operator.

Quantum gates, however, must be unitary operators, so instead, we work within the UCC framework.

1. Background

$$|\psi\rangle = e^{\hat{T}} |\phi_0\rangle$$

Where \hat{T} is now an **anti-Hermitian** operator, and $e^{\hat{T}}$ is unitary.

In general, we can prepare exact electronic states by applying a sequence of k parametrised unitary operators to our reference state.

$$|\psi\rangle = \prod_i^k U_i(\theta_i) |\phi_0\rangle$$

Where $U_i(\theta_i)$ is a parametrised unitary operator

The parameters θ_i are then optimised to find the ground state energy.

General fermionic single and double excitation operators are defined as,

$$a_q^\dagger a_p \text{ and } a_r^\dagger a_s^\dagger a_q a_p$$

Exciting one electron from p to q , and two electrons from p, q to r, s respectively.

Taking a linear combination of these, we obtain **anti-Hermitian** fermionic single and double excitation operators.

$$\begin{aligned}\hat{\kappa}_p^q &= a_q^\dagger a_p - a_p^\dagger a_q \\ \hat{\kappa}_{pq}^{rs} &= a_r^\dagger a_s^\dagger a_q a_p - a_p^\dagger a_q^\dagger a_s a_r\end{aligned}$$

Such that upon exponentiating, we obtain **unitary** operators.

$$U_p^q = e^{\hat{\kappa}_p^q} \quad U_{pq}^{rs} = e^{\hat{\kappa}_{pq}^{rs}}$$

Recalling the Jordan-Wigner encoding for the creation and annihilation operators,

1. Background

$$\hat{a}_j^+ = \frac{1}{2}(X - iY) \otimes Z_{j-1}^{\rightarrow} \quad \hat{a}_j = \frac{1}{2}(X + iY) \otimes Z_{j-1}^{\rightarrow}$$

The anti-Hermitian fermionic single and double excitation operators κ_p^q and κ_{pq}^{rs}

$$\begin{aligned} F_p^q &= \frac{i}{2}(Y_p X_q - X_p Y_q) \prod_{k=p+1}^{q-1} Z_k \\ F_{pq}^{rs} &= \frac{i}{8}(X_p X_q Y_s X_r + Y_p X_q Y_s Y_r + X_p Y_q Y_s Y_r + X_p X_q X_s Y_r - \\ &\quad Y_p X_q X_s X_r - X_p Y_q X_s X_r - Y_p Y_q Y_s X_r - Y_p Y_q X_s Y_r) \prod_{k=p+1}^{q-1} Z_k \prod_{l=r+1}^{s-1} Z_l \end{aligned}$$

Multiplying by θ and exponentiating yields the parametrised unitary qubit operators,

$$\begin{aligned} U_p^q(\theta) &= \exp \left(i \frac{\theta}{2} (Y_p X_q - X_p Y_q) \prod_{k=p+1}^{q-1} Z_k \right) \\ U_{pq}^{rs}(\theta) &= \exp \left(i \frac{\theta}{8} (X_p X_q Y_s X_r + \dots - Y_p Y_q Y_s X_r - Y_p Y_q X_s Y_r) \prod_{k=p+1}^{q-1} Z_k \prod_{l=r+1}^{s-1} Z_l \right) \end{aligned}$$

To summarise, we constructed anti-Hermitian single and double excitation operators from a linear combination of fermionic excitation operators,

$$\hat{\kappa}_p^q = a_q^\dagger a_p - a_p^\dagger a_q \quad \hat{\kappa}_{pq}^{rs} = a_r^\dagger a_s^\dagger a_q a_p - a_p^\dagger a_q^\dagger a_s a_r$$

We then mapped these to qubit operators using the Jordan-Wigner transformation,

$$\hat{\kappa}_p^q \xrightarrow{\text{JW}} F_p^q \quad \hat{\kappa}_{pq}^{rs} \xrightarrow{\text{JW}} F_{pq}^{rs}$$

And finally, we exponentiated to yield the parametrised unitary qubit operators.

$$U_p^q(\theta) = e^{\theta_p^q F_p^q} \quad U_{pq}^{rs}(\theta) = e^{\theta_{pq}^{rs} F_{pq}^{rs}}$$

1. Background

1.3 Fermion-Qubit Encodings

The form of the occupation number representation basis suggests the following identification between electronic states and qubit states.

$$|f_{n-1} \dots f_0\rangle \rightarrow |q_{n-1} \dots q_0\rangle$$

That is, we allow each qubit to store the occupation number of a given spin-orbital.

We must map the fermionic creation and annihilation operators onto qubit operators.

$$\hat{a}^\dagger \rightarrow \hat{Q}^+ \quad \hat{a} \rightarrow \hat{Q}$$

And these operators must behave in the same way as their fermionic analogues.

$$\begin{aligned} \hat{Q}^+ |0\rangle &= |1\rangle & \hat{Q}^+ |1\rangle &= 0 \\ \hat{Q} |1\rangle &= |0\rangle & \hat{Q} |0\rangle &= 0 \end{aligned}$$

Note that we must also preserve the fermionic anti-commutation relations in the qubit operators.

$$\begin{aligned} \{\hat{Q}_j, \hat{Q}_k\} &= 0 & \{\hat{Q}_j^\dagger, \hat{Q}_k^\dagger\} &= 0 \\ \{\hat{Q}_j, \hat{Q}_k^\dagger\} &= \delta_{jk} \end{aligned}$$

This ensures the fermionic exchange anti-symmetry of our qubit state vector.

We can do this using the **Jordan-Wigner** transformation by expressing the fermionic operators as a linear combination of the Pauli matrices.

We can see that these do indeed behave in the same way as their fermionic analogues,

1. Background

$$\begin{aligned}\hat{Q}^+ &= |1\rangle \langle 0| = \frac{1}{2}(X - iY) \\ \hat{Q} &= |0\rangle \langle 1| = \frac{1}{2}(X + iY)\end{aligned}$$

Figure 1.1: Single qubit creation and annihilation operators.

$$\begin{aligned}\hat{Q}^+ |0\rangle &= (|1\rangle \langle 0|) |0\rangle = |1\rangle & \hat{Q}^+ |1\rangle &= (|1\rangle \langle 0|) |1\rangle = 0 \\ \hat{Q} |1\rangle &= (|0\rangle \langle 1|) |1\rangle = |0\rangle & \hat{Q} |0\rangle &= (|0\rangle \langle 1|) |0\rangle = 0\end{aligned}$$

When dealing with **multiple-qubits**, we must also account for the occupation parity of the qubits preceding the target qubit j .

$$a_j^\dagger |f_{n-1} \dots f_{j+1}, 0, f_{j-1} \dots f_0\rangle = (-1)^{\sum_{s=0}^{j-1} f_s} |f_{n-1} \dots f_{j+1}, 1, f_{j-1} \dots f_0\rangle$$

We do this by introducing a string of Pauli Z operators that computes the parity of the qubits preceding the target qubit.

$$\hat{a}_j^+ = \frac{1}{2}(X - iY) \prod_{k=1}^{j-1} Z_k \quad \hat{a}_j = \frac{1}{2}(X + iY) \prod_{k=1}^{j-1} Z_k$$

Where \prod is the tensor product.

A more compact notation is,

$$\hat{a}_j^+ = \frac{1}{2}(X - iY) \otimes Z_{j-1}^{\rightarrow} \quad \hat{a}_j = \frac{1}{2}(X + iY) \otimes Z_{j-1}^{\rightarrow}$$

Where Z_i^{\rightarrow} is the parity operator with eigenvalues ± 1 , and ensures the correct phase is added to the qubit state vector.

$$Z_i^{\rightarrow} = Z_i \otimes Z_{i-1} \otimes \dots \otimes Z_0$$

For instance, the creation operator a_3^\dagger maps to the following Pauli string,

1. Background

$$\begin{aligned}\hat{a}_3^\dagger &= \frac{1}{2}(X_3 - iY_3) \otimes Z_2 \otimes Z_1 \otimes Z_0 \\ \hat{a}_3^\dagger &= \frac{1}{2}(X_3 \otimes Z_2 \otimes Z_1 \otimes Z_0) - \frac{1}{2}i(Y_3 \otimes Z_2 \otimes Z_1 \otimes Z_0)\end{aligned}$$

Usually we drop the subscript specifying the orbital acted on.

1. Background

1.4 DISCO-VQE

Excitation Operators in ZXC

Let's look again at the parametrised single-body unitary operator,

$$U_p^q(\theta) = \exp \left(i \frac{\theta}{2} (Y_p X_q - X_p Y_q) \prod_{k=p+1}^{q-1} Z_k \right)$$

$$U_p^q(\theta) = \left(\exp \left[i \frac{\theta}{2} Y_p X_q \prod_{k=p+1}^{q-1} Z_k \right] \right) \left(\exp \left[-i \frac{\theta}{2} X_p Y_q \prod_{k=p+1}^{q-1} Z_k \right] \right)$$

The first exponential term can be implemented by the following phase gadget.

$$\exp \left(i \frac{\theta}{2} Y_p X_q \prod_{k=p+1}^{q-1} Z_k \right)$$

Whilst the second exponential term can be implemented by the phase gadget.

$$\exp \left(-i \frac{\theta}{2} X_p Y_q \prod_{k=p+1}^{q-1} Z_k \right)$$

Together, they constitute the single-body unitary excitation operator $U_p^q(\theta)$

By defining the ordering of spin-orbitals such that adjacent spin-orbitals share the same spatial orbital, adjacent single-body operators commute.

$$[\hat{\kappa}_p^q, \hat{\kappa}_{p+1}^{q+1}] = 0$$

The same is therefore true for the resulting qubit operators,

$$[F_p^q, F_{p+1}^{q+1}] = 0$$

$$p, q \in \text{even} \quad p+1, q+1 \in \text{odd}$$

This allows us to define the parametrised unitary qubit operators in terms of spin-adapted excitation operators.

1. Background

$$U_p^q(\theta) = \exp \left[\theta \left(F_p^q + F_{p+1}^{q+1} \right) \right]$$

In other words, since F_p^q and F_{p+1}^{q+1} commute, we can think of them as a single operator with a single parameter.

Chapter 2

Phase Gadgets

2.1 Phase Gadgets

1. zx representation
2. algebraic structure
3. relation to chemistry
4. phase gadget decomposition / ladder / bricklayering

2.2 Pauli Gadgets

2.3 Commutation Relations

Chapter 3

Pauli Gadgets

$$C \in \text{Clifford} \quad P \in \text{Pauli}$$

$$\text{prove: } Ce^P C^\dagger = e^{CPC^\dagger}$$

$$CP^n C^\dagger = (CPC^\dagger)^n$$

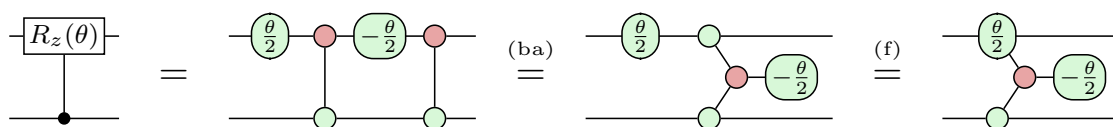
$$Ce^P C^\dagger = C \sum_{n=0}^{\infty} \left(\frac{P^n}{n!} \right) C^\dagger = \sum_{n=0}^{\infty} \frac{CP^n C^\dagger}{n!} = \sum_{n=0}^{\infty} \frac{(CPC^\dagger)^n}{n!}$$

Chapter 4

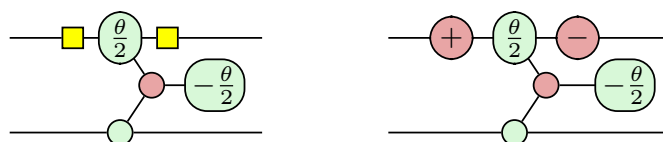
Controlled Rotations

4.1 Singly-Controlled Rotations

Singly-controlled Z rotation.



Singly-controlled X and Y rotations obtained by conjugating the control qubit.



4.2 Doubly-Controlled Rotations

hello world

4.3 Triply-Controlled Rotations

hello world hello world

Chapter 5

ZxFermion Package

ZxFermion is a Python package built on top of PyZX designed for the manipulation and visualisation of circuits of Pauli gadgets. With built-in Clifford tableau logic using Stim, ZxFermion allows users to quickly implement proofs and test ideas.

VQE algorithms used in quantum chemistry often utilise the UCC framework in which excitation operators have a natural representation as Pauli gadgets. ZxFermion provides a comprehensive toolset designed to be used in a Jupyter notebook environment. Export functionality can be used to generate research paper quality diagrams.

5.1 Creating Gadgets

5.2 Creating Circuits of Gadgets

5.3 Pauli & Clifford Algebra

```
from zxfermion.gates import X, XPlus, XMinus, Z, ZPlus
```

```
XPlus + XMinus  
>> Identity
```

5.4 Architecture-Aware Circuit Extraction

Appendices

Bibliography

- [1] Burton, H. G. A., Marti-Dafcik, D., Tew, D. P. & Wales, D. J. Exact electronic states with shallow quantum circuits from global optimisation. *npj Quantum Information* **9** (2023).
- [2] Yeung, R. Diagrammatic design and study of ansätze for quantum machine learning (2020). 2011.11073.
- [3] McClean, J. R., Romero, J., Babbush, R. & Aspuru-Guzik, A. The theory of variational hybrid quantum-classical algorithms. *New Journal of Physics* **18**, 023023 (2016).
- [4] Kirby, W. M. & Love, P. J. Variational quantum eigensolvers for sparse hamiltonians. *Phys. Rev. Lett.* *127*, 110503 (2021) **127**, 110503 (2020). 2012.07171.